



Pliocene and Early Pleistocene glaciation and landscape evolution on the Patagonian Steppe, Santa Cruz province, Argentina

John J. Clague^{a, *}, Rene W. Barendregt^b, Brian Menounos^c, Nicholas J. Roberts^{a, d}, Jorge Rabassa^e, Oscar Martinez^f, Bettina Ercolano^g, Hugo Corbella^h, Sidney R. Hemmingⁱ

^a Department of Earth Sciences, Simon Fraser University, 8888 University Drive, Burnaby, BC, V5A 1S6, Canada

^b Department of Geography, University of Lethbridge, 4401 University Drive, Lethbridge, AB, T1K 3M4, Canada

^c Geography Program and Natural Resources and Environmental Studies Institute, University of Northern British Columbia, 3333 University Way, Prince George, BC, V2N 4Z9, Canada

^d Mineral Resources Tasmania, Department of State Growth, 30 Gordons Hill Road, PO Box 56, Rosny Park TAS, 7018, Australia

^e CADIC-CONICET, Bernardo Houssay # 200, 9410 Ushuaia, Tierra del Fuego, Argentina

^f Facultad de Ciencias Naturales, Universidad Nacional de la Patagonia San Juan Bosco, Sarmiento 849, Esquel, Chubut, Argentina

^g Instituto Ciencias del Ambiente Sustentabilidad y Recursos Naturales, Universidad Nacional de Tierra del Fuego, Avenida Gobernador Gregores y Piloto "Lero" Rivera, 9400, Río Gallegos, Argentina

^h Museo Argentino de Ciencias Naturales CONICET, Avenida Ángel Gallardo 490, Buenos Aires, Argentina

ⁱ Earth and Environmental Sciences and Lamont-Doherty Earth Observatory, Columbia University, 413 Comer, 61 Route 9W, PO Box 1000, Palisades, NY, 10964–8000, USA

ARTICLE INFO

Article history:

Received 21 June 2019

Received in revised form

2 October 2019

Accepted 7 October 2019

Available online 19 November 2019

Keywords:

Glaciation

Cenozoic

Landscape evolution

Geomorphology

Radiogenic isotopes

Paleomagnetism

Patagonia

Argentina

South America

ABSTRACT

At least seven late Pliocene tills cap plateaus (mesetas) south of Lago Viedma, just east of the Andes in Argentine Patagonia. Chronologic constraints on the tills are provided by $^{40}\text{Ar}/^{39}\text{Ar}$ ages and magnetic polarities on associated basalt flows and sediments. The tills were deposited by piedmont glaciers that reached at least 80 km east of the crest of the Andes and flowed on a low-relief surface sloping gently downward in that direction. The oldest of the tills is about 3.6 Ma old. Glacial deposits dating to the Pliocene-Pleistocene transition are present at least 40 km beyond the east limit of the Pliocene tills at Lago Viedma, and tills of similar age occur at Condor Cliff in the Río Santa Cruz valley to the southeast. A sequence of at least seven Early Pleistocene (2.1–1.1 Ma) tills is present between basalt flows in the Cerro del Fraile meseta south of Lago Argentino. The glaciers that deposited these Early Pleistocene tills reached far beyond the Marine Isotope Stage 2 limit in the Río Santa Cruz valley. Based on positions, extents, and ages of the un-deformed, basalt-capped mesetas flanking Lago Viedma, we conclude that the topography in this area was profoundly changed during the Pleistocene – the low to moderate relief Pliocene surface was deeply incised by glaciers that became increasingly confined to, and flowed within, troughs. The valley floors today are up to 1350 m below the late Pliocene surface.

© 2019 The Authors. Published by Elsevier Ltd. This is an open access article under the CC BY-NC-ND license (<http://creativecommons.org/licenses/by-nc-nd/4.0/>).

1. Introduction

A notable feature in Earth's history is the gradual change in conditions favorable for continental glaciation during the Pliocene

and Early Pleistocene (3.5–1.5 Ma). Factors that could account for this change include decreasing concentrations of atmospheric CO_2 (Bartoli et al., 2011), closing of the Isthmus of Panama (Haug and Tiedemann, 1998), and orogenic events (Ruddiman and Kutzbach, 1989). Although these forcing mechanisms may explain intensification of glaciation in the Northern Hemisphere, a decrease in CO_2 is the only factor that can explain progressive expansion of the Greenland Ice Sheet (Lunt et al., 2008). Drawdown of CO_2 or changes in ocean circulation driven by variability in ice around Antarctica (Hill et al., 2017) could account for late Pliocene glacier expansion in the Southern Hemisphere (Clapperton, 1979; Roberts

* Corresponding author.

E-mail addresses: jclague@sfu.ca (J.J. Clague), barendregt@uleth.ca (R.W. Barendregt), Brian.Menounos@unbc.ca (B. Menounos), Nick.Roberts@stategrowth.tas.gov.au (N.J. Roberts), jrabassa@gmail.com (J. Rabassa), oam1958@gmail.com (O. Martinez), bercolano@yahoo.com.ar (B. Ercolano), hcorbel@yahoo.com.ar (H. Corbella), sidney@ldeo.columbia.edu (S.R. Hemming).

et al., 2017). Most of the evidence of glacier expansion over the past 5.0 Ma, however, has been derived from marine sediments, which record global ice volumes (e.g. Lisiecki and Raymo, 2005). Glacier and fluvial erosion has removed most landforms and deposits that could be used to document past glacier events on land.

The Patagonian Steppe is one of the few areas in the world that preserves evidence of Pliocene and Early Pleistocene glaciations because it is arid and supports widespread basalt flows ranging in age from the late Miocene to Holocene. Evidence for Pliocene glaciations in Patagonia was first presented by Feruglio (1944) at Cerro del Fraile south of Lago Argentino (Fig. 1), although subsequent $^{40}\text{K}/^{40}\text{Ar}$ (Fleck et al., 1972) and $^{40}\text{Ar}/^{39}\text{Ar}$ (Ton That et al., 1999; Singer et al., 2004) dating of associated volcanic rocks showed that these glaciations are of Early Pleistocene age. Later Fleck et al. (1972), Mercer et al. (1973), Mercer (1976, 1983), Strehlin (1995), Wenzens et al. (1996, 1998), Schellmann (2000), and Wenzens (2000) identified and dated Pliocene glacial deposits elsewhere in

the Southern Andes. This work showed that there were extensive piedmont glaciations in the Pliocene and that some of them extended as far east as major Pleistocene glacier lobes (see Rabassa, 2008 for a complete review of research on Pliocene and Pleistocene glaciations in Patagonia).

The work of John Mercer, published more than 40 years ago (Mercer et al., 1973; Mercer, 1976), was particularly important in establishing the ages and limits of late Pliocene glaciations in Argentine Patagonia. Mercer's and our study sites on mesetas north of Lago Viedma (Fig. 1) are many tens of kilometres east of the crest of the Andes and at elevations requiring the presence of a substantial ice sheet over the Southern Andes. The key evidence presented by Mercer is the presence of a lodgement till between two flat-lying basalt flows near the top of a thick Pliocene volcanic sequence at Meseta Chica and Meseta Desocupada (Fig. 1). Whole-rock $^{40}\text{K}-^{40}\text{Ar}$ ages on flows directly below and above the till indicated that it was about 3.5 million years old (Supplement Table S1).

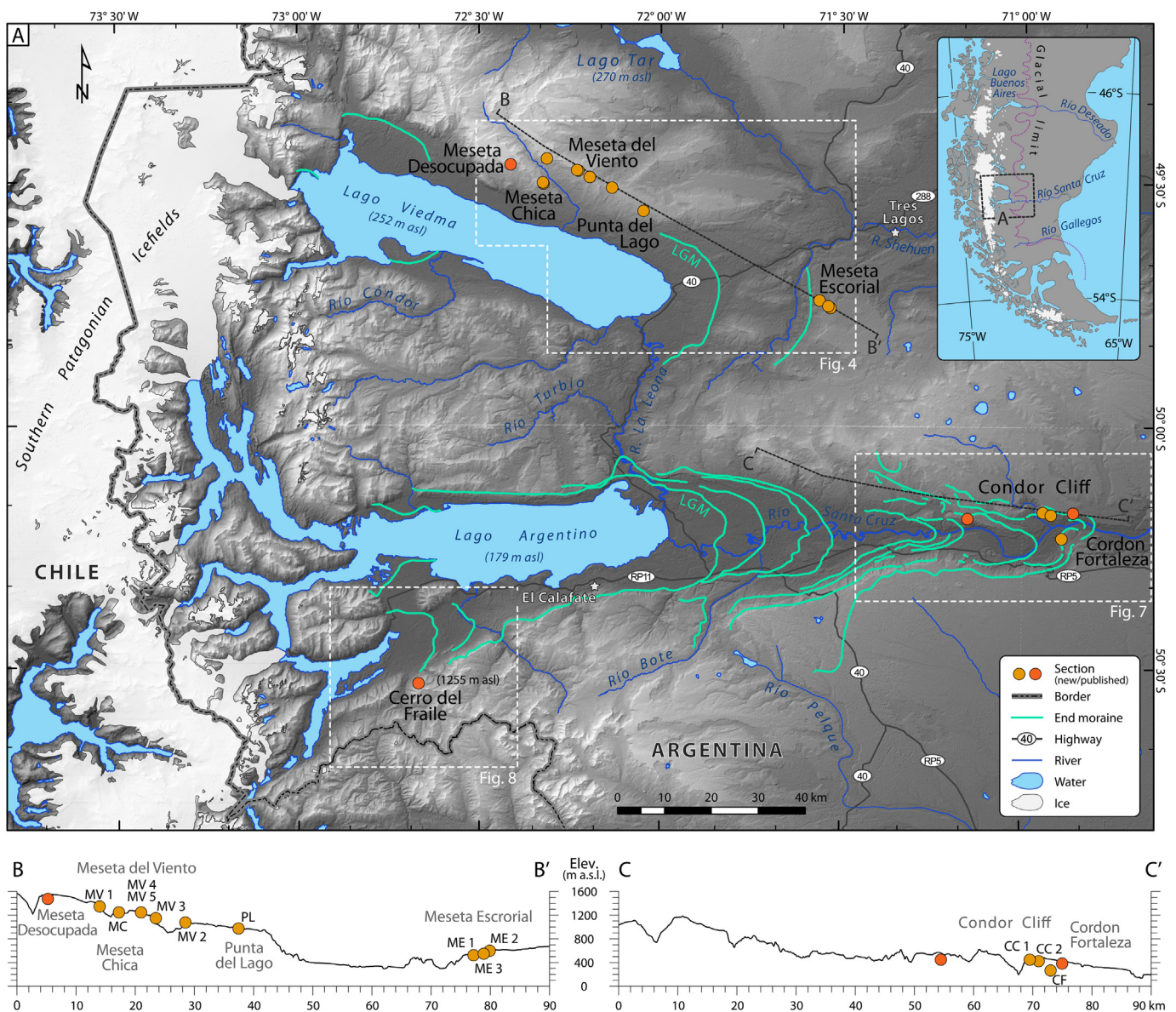


Fig. 1. Study area overview. A) Location map showing sites and physiography. Valley-bottom moraines are, in part, from Mercer (1976), Schellmann (1998), and Wenzens (2006). B) Topographic profile showing elevations of sections in the Lago Viedma basin. C) Topographic profile showing elevations of sections in the Río Santa Cruz valley. Base map and profiles are derived from ASTER GDEM 2 elevation data produced by METI and NASA.

Mercer's work raised important questions about inter-hemispheric correlations of late Cenozoic glacial records. At the time he worked in Patagonia, no evidence had been presented in the literature for Pliocene glaciation in North America outside the St. Elias Mountains (Denton and Armstrong, 1969), and even there the evidence could be explained by only a minor expansion of glaciers in this heavily ice-covered mountain range (Eyles and Eyles, 1989). More recently, the time of the first expansion of an ice sheet in western Canada has been dated to about 2.7 Ma (Duk-Rodkin et al., 2010; Barendregt et al., 2010; Hidy et al., 2013), about 800,000 years after the Pliocene event that Mercer documented, and little evidence has been presented for a Laurentide ice sheet this old. Gao et al. (2012) have argued for one, but their evidence, in our opinion, is not compelling and requires confirmation.

In view of the significance of Mercer's findings, we revisited his field sites and studied others on the mesetas north of Lago Viedma. We also visited sites east of Lago Viedma and in the Río Santa Cruz valley to the southeast that previous researchers have suggested were glaciated in latest Pliocene or earliest Pleistocene time. We used the $^{40}\text{Ar}/^{39}\text{Ar}$ dating method to obtain new ages on critical basalt flows bounding tills, determined the magnetic polarities of those flows and interbedded sediments, and considered the paleotopographic implications of Pliocene glacial events to younger Pleistocene ones.

2. Setting

Our main study area lies east of the crest of the Southern Andes and north of Lago Viedma at about 49.5°S (Fig. 1). At this latitude, the Andean crest averages about 2000 m above sea level (asl), and the highest peak (Cordon Mariano Moreno) has an elevation of 3490 m asl. The Southern Patagonian Icefield covers this part of the Andes, with outlet glaciers that calve into Pacific fjords to the west and fjord lakes to the east. One of these glaciers, Glaciar Viedma, calves into the west end of Lago Viedma.

Rocks underlying the Magellan foreland basin in the Lago Viedma area are relatively undeformed Lower Cretaceous and Tertiary marine and continental sedimentary rocks up to 8 km thick (Coutand et al., 1999; Gorrington, 2008). An unconformity separates the Cretaceous rocks from underlying, more highly deformed Jurassic basement rocks (Coutand et al., 1999). To the west, in the Andean fold-and-thrust belt, late Paleozoic sedimentary and metamorphic rocks, Jurassic volcanic rocks, and Lower Cretaceous and Tertiary sedimentary rocks form thick sequences that have been involved in thick- and thin-skinned brittle deformation (Riccardi, 1988; Coutand et al., 1999). Mesozoic to Miocene calc-alkaline granitic rocks of the Patagonian Batholith are present along the axis of the range.

Plateaus (mesetas) consisting of late Miocene and early Pliocene basalt flows are important elements of the landscape east of the Andes and south of 46.5°S , including the Lago Viedma area. A 'main plateau' sequence of late Miocene (12–7 Ma) age, which forms the highest mesetas, comprises tholeiitic basalts and basaltic andesites (Ramos and Kay, 1992; Gorrington et al., 1997; Gorrington and Kay, 2001). Inset into these surfaces are lower mesetas developed on Pliocene and Early Pleistocene (5–2 Ma) 'post-plateau' alkaline basalts and hawaiites. Both the main plateau and post-plateau lavas have an intra-plate ocean island basalt affinity, both in trace elements and isotopic composition. This extended period of volcanism is thought to have resulted from opening of an asthenospheric slab window due to the oblique collision of the Chilean Pacific ridge with the Chilean trench (Forsythe et al., 1986; Ramos, 1989; Ramos and Kay, 1992; Murdie et al., 1993; Gorrington et al., 1997; Ramos and Ghiglione, 2008).

Lago Viedma (252 m asl) extends 79 km east-southeast across

the Patagonian plains from the Andean front. The basin in which the lake sits has been excavated by glacier ice flowing eastward from the Andes during repeated glaciations. Lateral and end moraines formed during these glacial events are nested around the lake, increasing in age away from the lakeshore and at progressively higher elevations on the slopes of the mesetas to the north and south. Deposits of older glaciations are also preserved on mesetas well east of Lago Viedma and in the Río Santa Cruz valley to the south (Mercer, 1976; Wenzens et al., 1996, 1998; Schellmann, 2000; Wenzens, 2000).

Our primary study sites are Meseta Chica, Meseta del Viento, Meseta Escorial, and Condor Cliff (Fig. 1). We visited Mercer's Meseta Chica locality to collect new samples for $^{40}\text{Ar}/^{39}\text{Ar}$ dating and magnetic polarity determination. The sites on Meseta del Viento were not previously reported by Mercer and are of importance because we found evidence there for multiple Pliocene glaciations. Glacial deposits on Meseta Escorial, east of Lago Viedma, were first mapped by Wenzens et al. (1996, 1998). We visited his key sites and obtained new $^{40}\text{Ar}/^{39}\text{Ar}$ ages on basalt flows that bear on old glaciations in that area. We also examined sections at Condor Cliff in the Río Santa Cruz valley, one of Mercer (1976)'s key study sites (Supplement Table S1). We describe landforms of Pleistocene glaciations nested below the meseta surface and discuss their ages in relation to dated deposits of multiple Early and Middle Pleistocene glaciations recorded in the flat-lying basaltic sequence at Cerro del Fraile south of Lago Argentino (Fig. 1; Supplement Table S1) reported by Fleck et al. (1972), Mercer (1976), and Singer et al., 2004. Finally, we discuss the implications of our data and those of previous researchers for large-scale landscape change, including topographic inversion, during the Pleistocene Epoch.

3. Methods

Our study is based on field mapping and sampling done in the austral summers of 2013 and 2014. Mapping was done using a combination of Landsat ETM+ images (30 m resolution; Global Land Cover Facility, www.landcover.org) and images displayed in Google Earth (2.5–15 m resolution; Cnes/SPOT, Digital Globe, and TerraMetrics images). We refined map polygons using 1-arcsecond Shuttle Radar Topographic (SRTM v3) elevation data (~30 m resolution; www.earthdata.nasa.gov).

3.1. Field work

We described sections based on lithology, texture, structure, colour, clast size and shape, weathering features, diamicton fabric, and the nature of contacts. Unit boundaries were defined at contacts indicating depositional hiatuses or major changes in material properties. We measured unit thicknesses and heights of key features above unit bases with a handheld laser rangefinder, and stratal thicknesses and sizes of large clasts with a graduated metric scale.

We collected six or more oriented cylindrical rock cores from basalt flows with a portable gasoline-powered rock drill used for standard paleomagnetic work. In some cases, oriented blocks of basalt were collected and later drilled. We trimmed the cores with a rock saw to produce 2.2-cm-long specimens. For sediment units, we collected six or more samples by inserting polycarbonate plastic cylinders (2.1 cm inside diameter, 1.8 cm inside length) into horizontally bedded lenses of silt or fine to very fine sand. Where such lenses were absent, we collected samples from the fine-grained matrix of diamicton, avoiding granules and pebbles. Samples were stored in magnetic shields following field collection.

3.2. Paleomagnetism

We made magnetic measurements in the paleomagnetic laboratory at the University of Lethbridge. Magnetic susceptibility was measured with a Sapphire Instruments (SI-2B) susceptibility meter. We measured the magnetization of each sample with an AGICO JR-6A spinner magnetometer prior to demagnetization and again after each level of stepwise demagnetization. Samples were stored in magnetic shields between measurements.

A pilot sample from each sample group was exposed to alternating field (AF) demagnetization in an ASC Scientific D-2000 demagnetizer with a three-axis manual tumbler at 10–20 mT steps (up to 200 mT). For basalt samples, a second pilot from the same core was thermally demagnetized at 100, 200, 300, 400, 500, and 550 °C, and in some cases 575, 600, 625, and 650 °C using an ASC Model TD48 dual-chamber thermal demagnetizer to confirm that AF demagnetization was sufficient to resolve their thermal remanent magnetization. Remaining sediment and basalt samples were then subjected to stepwise AF demagnetization generally at 20, 40, 60, and 80 mT, and in some cases additionally at 100, 120, or up to 200 mT if strongly magnetized (Supplement Figs. S1 and S2). Median destructive fields typically ranged from 20 to 80 mT for the magnetite-bearing sediments and from 40 to 80 mT for basalts. Thermal demagnetization of basalt samples revealed a steep decrease in magnetization between 400 and 600 °C, commonly at 550 or 575 °C, indicating that magnetite is the dominant remanence carrier.

We determined paleomagnetic directions (Table 1) for each sample by principle component analysis (Kirschvink, 1980) using Remasoft v. 3.0. We calculated mean remanence directions by group and polarity based on principle components of individual samples using the group statistics function in Remasoft v. 3.0 (Fig. 2 and Supplement Fig. S3). Polarities were assigned to each sample group based on mean directions. Mean directions are considered to be of high quality where α_{95} values are $\leq 15^\circ$. As a test of significance, we compared the inclination mean for each sample group to the geocentric axial dipole (GAD) field inclination (-67° and 67° for, respectively, normal and reversed fields) for the Lago Viedma sampling latitude ($\sim 50^\circ$ S). The mean inclination is expected to be similar to the GAD, and the two directions cannot be discriminated at the 5% significance level if the GAD is within α_{95} of the measured mean direction (Butler, 1992). For our sample sites, there is good coherence of the group mean directions, and the group mean inclination (63°) is only marginally shallower than the GAD (67°).

3.3. $^{40}\text{Ar}/^{39}\text{Ar}$ dating

We processed basalt samples selected for $^{40}\text{Ar}/^{39}\text{Ar}$ dating at the AGES (Argon Geochronology for the Earth Sciences) laboratory at Lamont-Doherty Earth Observatory (Columbia University). Samples were crushed and wet-sieved, and the clean and fine groundmass was hand-picked under a binocular microscope from the 300–500 μm fraction. Groundmass samples were co-irradiated with either Fish Canyon or Alder Creek sanidine for 8 h at the US Geological Survey TRIGA reactor in Denver, Colorado, using cadmium shielding. We calculated ages (Table 1) assuming an age of 28.201 ± 0.046 Ma for Fish Canyon sanidine (Kuiper et al., 2008) or 1.195 Ma for Alder Creek sanidine, consistent with our internal runs of Alder Creek against Fish Canyon samples. Monitor samples were measured from the gas derived from single-step fusion with a 30 W Merchantek CO_2 laser. Groundmass samples were placed in tantalum tubes and were incrementally heated using progressively higher power steps with a 50 W Photon Machines Diode laser. Argon measurements were made on a VG5400 noble gas mass spectrometer after the gas was passed through two warm GP50

getters in the extraction line to remove active gasses. The mass spectrometer is equipped with two unheated GP50 getters. We made measurements by peak-hopping into an analogue multiplier. The sensitivity of the system was monitored with the air pipette analyses. Argon isotopes were corrected for background and mass discrimination based on measurements of, respectively, blanks and airs. Mass discrimination and atmospheric corrections were made using the atmospheric composition from Lee et al. (2006). Corrections for nuclear interferences were made based on the production ratios from Dalrymple et al. (1981). The ratio of ^{40}Ar (the radiogenic argon) to ^{39}Ar was then used to calculate an age for each sample.

4. Results

We present our stratigraphic observations and geochronological and paleomagnetic data from oldest to youngest and approximately from north to south. We first describe sections at Mesta Chica and Meseta del Viento with evidence for recurrent late Pliocene glaciation. Next we describe sections at Condor Cliff, where there is evidence of late Pliocene and earliest Pleistocene glaciations. We then present evidence for glaciation near the Pliocene-Pleistocene boundary at Meseta Escorial. Finally, we briefly review the Cerro del Fraile section with its evidence for multiple glaciations spanning the period from about 2.2 Ma to 1.0 Ma. Fig. 3 summarizes the radiometric and polarity results from all sites. We elaborate on these results in the following sections.

4.1. Pliocene glacial deposits

The critical stratigraphy of the Meseta Chica and Meseta del Viento localities is shown in Fig. 4.

4.1.1. Meseta Chica

At Meseta Chica diamicton and very poorly sorted, sandy gravel lie between basalt flows near the top of a >50-m-thick sequence of flat-lying flows that unconformably overlie Upper Cretaceous sedimentary rocks (Fig. 5A and B). The diamicton is matrix-supported and contains striated and faceted, subangular to sub-rounded clasts up to about 1 m across. Like Mercer (1976), we interpret it to be till. Clast lithologies include basalt, andesite, argillite, sandstone, and quartz diorite. The basalt and sandstone clasts might be derived from rocks that crop out in the immediate area. The other clasts are sourced in the Andes, approximately 50 km to the west. The till is no more than 1.5 m thick at our study site and is sharply underlain and overlain by reversely magnetized basalt flows. A silt lens near the top of the till is reversely magnetized. Approximately 40 m of basalt, comprising about seven individual flows, underlie the till unit. No sediments were found at the contacts between these flows. Similarly, three flows (12 m in total thickness) above the till are not separated by sediments. The uppermost flow in the sequence, however, is capped by two matrix-supported diamicton units containing striated and faceted clasts of Andean provenance: a lower, 4-m-thick unit with clasts up to boulder size; and an upper, 9-m-thick, finer unit with clasts mainly of pebble and cobble size (Fig. 5C). A thin, normally magnetized silt bed separates the two till units. The two capping diamictons directly underlie the meseta surface. Most of the meseta surface, however, entirely lacks glacial sediments, even erratics. Till is limited to small areas that we infer to be swales on the meseta. The patchy distribution of glacial sediments speaks to the antiquity of these deposits.

The basalt flows bracketing the lowest till yielded $^{40}\text{Ar}/^{39}\text{Ar}$ ages of 3.61 ± 0.09 Ma (above) and 3.85 ± 0.10 Ma (below) (Table 1). These ages are slightly older than Mercer (1976)'s bracketing,

Table 1
Ar⁴⁰-Ar³⁹ ages and magnetic polarity data.

	Sample no. ^a	Location (°S °W)	Basalt age (Ma)/Sed. description	Laboratory no.	n _c ^b	n _u ^b	D (°)	I (°)	k	α ₉₅	Polarity	
Basalt flows	MC 1-1	49.50563 72.32331	3.61 ± 0.09	LV7-1 ^c	7	6	145	43	199	5	R	
	MC 1-2	49.50563 72.32331	3.85 ± 0.10	LV7-2 ^c	7	7	254	16	181	5	TR [‡]	
	MV 1-1	49.45395 72.31278	3.83 ± 0.01	17067-01 ^d								
	MV 1-2	49.45395 72.31278	3.75 ± 0.10	LV8-2 ^c	6	6	163	74	378	3	R	
	MV 2-1	49.51337 72.13384	3.61 ± 0.09	LV 2-1 ^c	6	6	81	79	231	4	R	
	MV 2-2	49.51337 72.13384	4.06 ± 0.10	LV-2-2 ^c	6	6	193	53	180	5	R	
	MV 3-0	49.49205 72.19506	ND		7	7	186.7	51.4	144	5.1	R	
	MV 3-1	49.49205 72.19506	4.28 ± 0.01	17070-01 ^d	8	7	185	57.5	474	4.7	R	
	MV 4	49.47803 72.22715	3.71 ± 0.01	17326-01 ^d								
	PL	49.56124 72.04675	4.05 ± 0.10	LV-13 ^c	6	6	175	54	473	3	R	
	ME 1	49.74337 71.56181	2.15 ± 0.10	LV-17 ^c	8	8	173	60	1262	2	R	
	ME 2-1	49.75898 71.53139	2.13 ± 0.09	LV-20 ^c	7	7	173	60	450	3	R	
	ME 3	49.75525 71.53773	2.23 ± 0.06	LV-21 ^c	7	7	174	59	2131	1	R	
	CC 1	50.17756 70.94070	2.71 ± 0.07	CCL-1 ^c	6	5	42	-45	432	4	N	
	CC 2-1	50.18278 70.91885	3.25 ± 0.08	17338-01 ^d	8	8	54	-86	116	5	N	
	CF	50.23122 70.88863	2.29 ± 0.06	CF0-1 ^c	7	7	1.9	22.6	136	5.2	TR [‡]	
		Mean of R flows					10	173	60	28	9	R
		Mean of N flows					2	43	-66	-	-	N
		Mean of all flows ^f					12	179	62	19	10	
		MC 1-3	49.50563 72.32331	Silt lens in till btn. two dated flows (MC 1-1 & MC 1-2)		8	6	186	56	192	5	R
Sediments	MC 2	49.50407 72.32348	Silt lens separating two tills capping meseta		12	5	356	-62	31	14	N	
	MV 1-3	49.45395 72.31278	Silt lens within lowest till		6	5	242	62	75	9	R	
	MV 1-5	49.47881 72.22602	Baked sediment between basalt flows		8	7	34	-44	13	22	N	
	MV 3-2	49.49205 72.19506	baked sands below lowest basalt (MV 3-1)		6	6	178.7	57.2	314	3.8	R	
	ME 2-2	49.74337 71.56181	Baked sandstone below surface basalt ME 2		6	6	171	67	92	7	R	
	CC 2-2	50.18278 70.91885	Baked silt and paleosol		6	5	194	-86	31	14	N [‡]	
		Mean of R sediment units					4	193	61	27	18	R
	Mean of N sediment units					3	21	-62	15	33	N	
	Mean of all sediment units ^f					7	197	63	24	12		
All	Overall mean of all R units					14	178	61	29	8	R	
	Overall mean of all N units					5	29	-64	15	21	N	
	Overall mean of all units ^f					19	186	63	21	7		

[‡] Group not used in calculation of means.

^a MC - Meseta Chica, MV - Meseta del Viento, PL - Punta del Lago, ME - Meseta Escorial, CC - Condor Cliff, CF - Cordon Fortaleza.

^b n_c - number of samples collected, n_u - number of samples used in statistical analysis.

^c Oregon State University Argon Laboratory.

^d AGES (Argon Geochronology for the Earth Sciences) Laboratory, Lamont-Doherty Observatory (Columbia University).

^e Very steep inclination accounts for anomalous declination value. Polarity based on inclination.

^f Irrespective of sign (upper hemisphere). GAD = -66.9° (N), 66.9° (R); PEF = 12° / -47°.

whole-rock ⁴⁰K/⁴⁰Ar ages of 3.55 ± 0.19 Ma and 3.50 ± 0.14 Ma (above) and 3.40 ± 0.03 Ma (below) at two locations about 400 m west of our study site. Mercer's age on the lower flow, however, must be too young because, as he reports, that flow is reversely magnetized and thus must be older than 3.588 Ma (the start of the Gauss Chron). Mercer obtained ⁴⁰K/⁴⁰Ar ages of 3.49 ± 0.08 Ma and 3.53 ± 0.05 Ma on basalt clasts in the till; these ages should be interpreted as maxima for the age of the glaciation that left the till, but again they appear to be too young given the magnetization of the bounding flows. Mercer also obtained two ⁴⁰K/⁴⁰Ar ages from basalt flows at Meseta Desocupada bracketing what he interpreted to be the same till as that exposed at Meseta Chica 8 km to the east-southeast - 3.48 ± 0.09 Ma (below) and 3.55 ± 0.07 Ma (above) (Fig. 4). Both ages appear to be a little too young as they are reversely magnetized and thus should be older than 3.588 Ma. In summary, the evidence considered together indicates the till 25 m below the surface at Meseta Chica was deposited during C2Ar and very likely during MIS Gi-2 or Gi-4 at about 3.7 Ma. MIS Gi-2 and Gi-

4 are the only significant cold intervals within C2Ar.

The two tills capping Meseta Chica have not been directly dated, although Mercer obtained a whole-rock ⁴⁰K/⁴⁰Ar age of 3.46 ± 0.22 Ma on the uppermost basalt flow on which they rest. This age is consistent with the normal polarity of the inter-till sediments above the uppermost flow. We tentatively assign the lower of the two surface tills at Meseta Chica to C2An.3n, between 3.588 Ma and 3.319 Ma; if so, it was deposited during either the MG-4 or MG-2 cold interval. The age of the upper of the two capping tills is uncertain as its polarity is unknown. If reversely magnetized, it likely was deposited during MIS M2, the single cold interval during the Mammoth subchron. This cold interval is recognized in climate records around the world and was colder and longer lived than either MIS Gi-2 or Gi-4.

4.1.2. Meseta del Viento

A section at the west margin of Meseta del Viento exposes seven

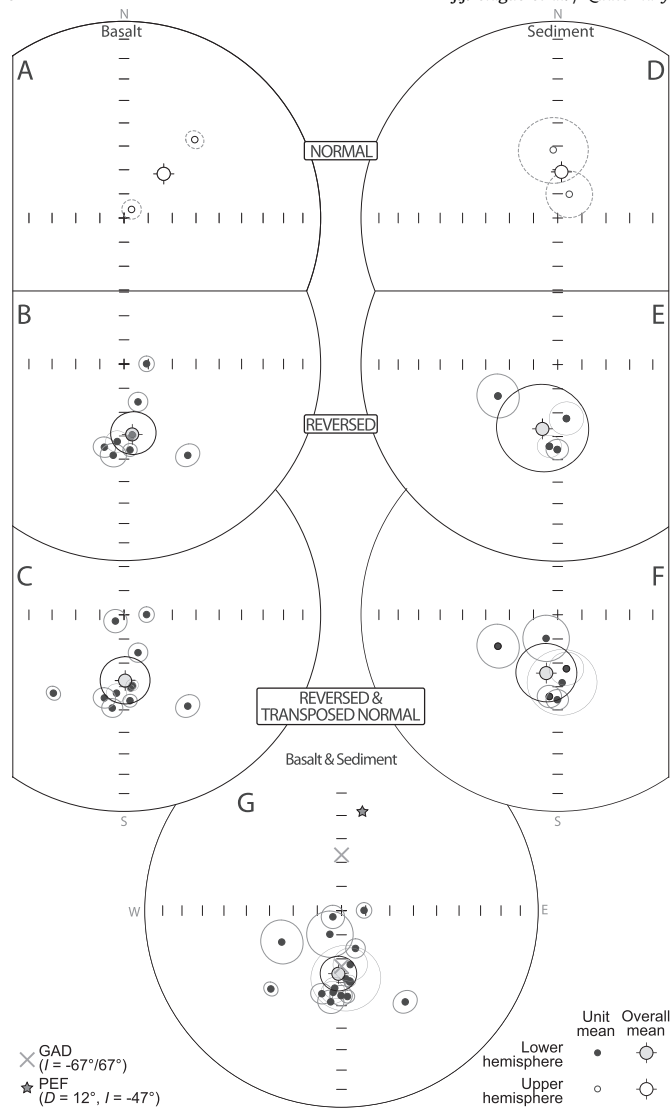


Fig. 2. Unit mean primary magnetic remanence directions by material type and polarity. Basalts: A) normally magnetized units; B) reversely magnetized units; C) all basalt units regardless of polarity, projected onto the lower hemisphere. Sediments: D) normally magnetized units; E) reversely magnetized units; F) all sediment units regardless of polarity, projected onto the lower hemisphere. G) All sample groups, regardless of material type or polarity, projected onto the lower hemisphere. See Table 1 for unit means. GAD, geocentric axial dipole; PEF, Earth's present magnetic field direction at the centre of the sample localities.

diamicton units that are separated by paleosols (site MV 1, Figs. 4 and 6). The diamictons are matrix-supported with about 25–35% stones ranging up to boulder size. Many of the stones are striated and faceted, and stones of Andean provenance are abundant. We interpret the diamictons to be tills. The paleosols are brownish to reddish zones, with colors that decrease in chroma and value downward. The prismatic structure of the soils and near-vertical fractures coated with clay minerals are interpreted to be pedogenic in origin. A silt lens in lowest of the seven diamicton units is reversely magnetized. As at Meseta Chica, the till sequence is restricted to a swale on the Meseta del Viento surface. Nearly the entire meseta lacks glacial sediments; even erratics are rare.

The seven diamicton units overlie a sequence of flat-lying basalt flows. The uppermost basalt flow is reversely magnetized and yielded a $^{40}\text{Ar}/^{39}\text{Ar}$ age of 3.83 ± 0.01 Ma (C2Ar: 4.184–3.588 Ma) (Table 1). It displays pillows, indicating that it erupted into water. Striations on its surface trend 70–90°. The next two lower basalt

flows are separated by a thin, baked silt bed. The flow beneath the silt bed is reversely magnetized and yielded a $^{40}\text{Ar}/^{39}\text{Ar}$ age of 3.75 ± 0.02 Ma, consistent with emplacement late during the Gilbert Chron (4.184–3.588 Ma). Given the radiometric ages and the magnetic polarity sequence, at least some of the seven tills above the flow sequence must be younger than the oldest of the three tills at the Meseta Chica site.

We also obtained $^{40}\text{Ar}/^{39}\text{Ar}$ ages on the upper part of the basalt sequence at several other sites on Meseta del Viento (Table 1). An upper, reversely magnetized flow at site MV 2 (Fig. 4) about 15 km southeast of our key study site returned an age of 3.61 ± 0.09 Ma, and a lower, reversely magnetized flow about 8 m below the meseta surface at the same site yielded an age of 4.06 ± 0.10 Ma. The younger of these two flows is at about the same elevation as the uppermost flow at site MV 1. We obtained a third age of 3.71 ± 0.01 Ma on the uppermost flow at site MV 4, 7 km southeast of site MV 1. These ages accord with those at site MV 1 and similarly suggest emplacement of the basalts during C2Ar. Finally, the lowest flow in the Meseta del Viento basalt sequence at site MV 3, 10 km southeast of site MV 1 is reversely magnetized and yielded an age of 4.28 ± 0.01 Ma, which likely places it in the C3n.1r polarity subchron. The entire flow sequence at Meseta del Viento spans about 700–800 ka.

4.1.3. Condor Cliff and Cordon Fortaleza

Condor Cliff is located in the valley of Río Santa Cruz, 87 km east-southeast of Lago Viedma (Fig. 1). We visited this site to build upon the observations and chronology of Mercer (1976), who inferred evidence of glaciation of latest Pliocene or earliest Pleistocene age there. The glacier that deposited this drift was separate from the Viedma lobe to the north, but the glacial sediments are similarly associated with flat-lying basalt flows. Our site lies at the limit of the oldest moraines and till in the Río Santa Cruz valley, nearly 200 km from the crest of the Andes.

At our study site, located 12 km east of Estancia Condor Cliff, a ~20-m-thick sequence of basalt flows is exposed in a steep escarpment on the north side of the Río Santa Cruz valley between about 405 and 425 m asl. (Fig. 7). The uppermost, till-capped flow in this sequence is normally magnetized and yielded a $^{40}\text{Ar}/^{39}\text{Ar}$ age of 2.71 ± 0.07 Ma. A normally magnetized flow about 10 m lower in the sequence yielded an age of 3.25 ± 0.08 Ma. Given its normal magnetization, the lower flow likely dates to shortly after 3.210 Ma.

The lower flow lies on up to 1 m of sediments that are likely of glacial origin. The sediments include matrix-supported diamicton, clast-supported gravel, and gravelly sand. Clasts are rounded to subrounded and up to 40 cm across; most are of Andean provenance. A normally magnetized paleosol within the sediment sequence suggests that the sediments record two periods of deposition separated by a period of non-deposition and soil formation. The paleosol includes clay-rich pedes with a near-vertical prismatic structure. The period of soil formation may span thousands of years given the cool climate of the region during the Pliocene. Up to 60 cm of stratified and massive scoria separate these sediments from the overlying basalt flow. Steeply dipping tongues of vesicular basalt extend upward from the base of the flow, indicating that the underlying sediments were wet when overridden by the lava. Although we cannot prove that the sediments at this locality are glacial, they lie at the all-time limit of glaciation in the Río Santa Cruz valley as mapped by Mercer (1976), Schellmann (1998), and Wenzens (2006).

Schellmann (2000) reports a K/Ar age of 3.46 ± 0.39 Ma on a basalt flow overlying till, which in turn directly overlies Early Miocene sedimentary rocks of the Santa Cruz Formation, at Condor Cliff. We were unable to find this exposure, but judging from

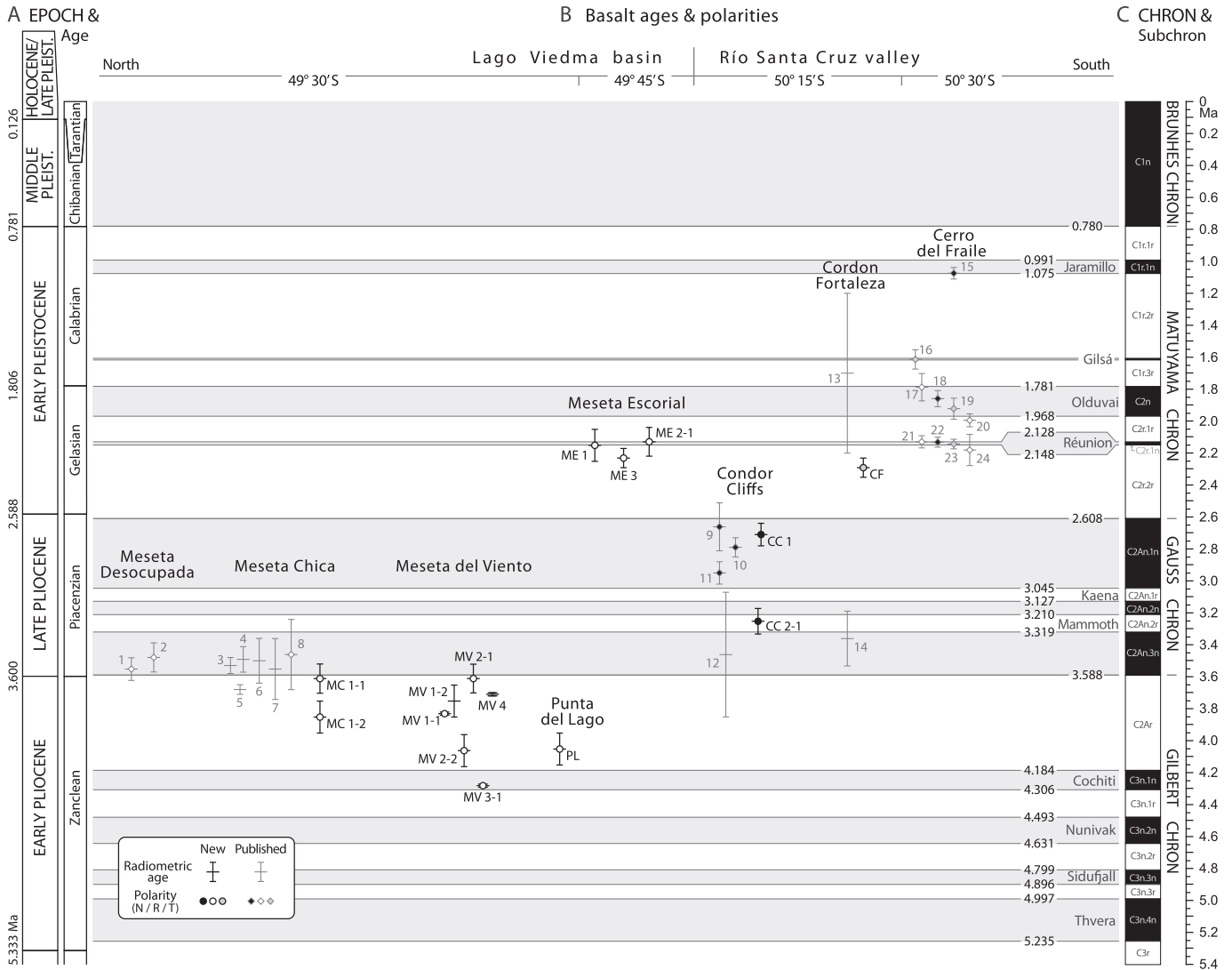


Fig. 3. Basalt geochronology based on radiometric and paleomagnetic analyses. Radiometric ages and paleomagnetic polarities are reported in Table 1 and Table S1 for, respectively, the current study (black lines and circles) and previous studies (grey lines and diamonds).

Schellmann's published sections the till lies at least 13 m below the diamicton described above at an elevation of about 402 m asl. Schellmann's till is about 280 m above the present-day floor of the Río Santa Cruz valley. The flow sequence above this lowest till is truncated along the steep north wall of the valley; there is no evidence that the flows spilled into a paleo-valley, and therefore we infer that the till directly overlying the Santa Cruz Formation, as reported by Schellmann, is older than our nearby inter-flow sediments.

A similar flow sequence crops out between about 225 and 320 m asl on the south side of the valley at Cordon Fortaleza (Fig. 7). We obtained a $^{40}\text{Ar}/^{39}\text{Ar}$ age of 2.29 ± 0.06 Ma on a flow with a transitional polarity about 45 m below the top of the flow sequence at Cordon Fortaleza and about 170 m below the highest Condor Cliff flow, which yielded an age of 2.71 ± 0.07 Ma. Schellmann (2000) reports a K/Ar age of 3.36 ± 0.17 Ma on basalt nearby and lower in the Cordon Fortaleza flow sequence at an elevation of about 225 m asl. We were unable to trace the flow sequence continuously down to this elevation at Cordon Fortaleza.

Given the spatial and age relations among these flows, we conclude that paleo-Río Santa Cruz was flowing in a valley with a

floor about 100 m above present river level sometime between 3.5 and 3.1 Ma. A nearly 100-m-thick stack of flows filled that valley by 2.7 Ma, followed by renewed incision of the valley of Río Santa Cruz in the Early Pleistocene.

4.2. Glaciation near the Pliocene-Pleistocene boundary

4.2.1. Meseta Escorial

A reversely magnetized basalt flow capped by erratic cobbles and boulders of Andean provenance underlies Meseta Escorial, 30 km east of Lago Viedma (Figs. 1 and 4). We obtained $^{40}\text{Ar}/^{39}\text{Ar}$ ages of 2.15 ± 0.10 Ma and 2.23 ± 0.06 Ma at two of the three sites that we sampled (Table 1). The flow has horizontal and inclined columns and fan-shaped joints indicating deposition in standing water, possibly in association with glacier ice. Large erratics and patches of till are present on slopes up to elevations at least 90 m above the surface of the flow.

The flow has a mean age of about 2.2 Ma, which is within the early Matuyama Chron (C2r.2r). It sharply overlies reversely magnetized, baked, laminated sand containing rounded to sub-rounded limestones up to 15 cm across. The clasts are largely non-

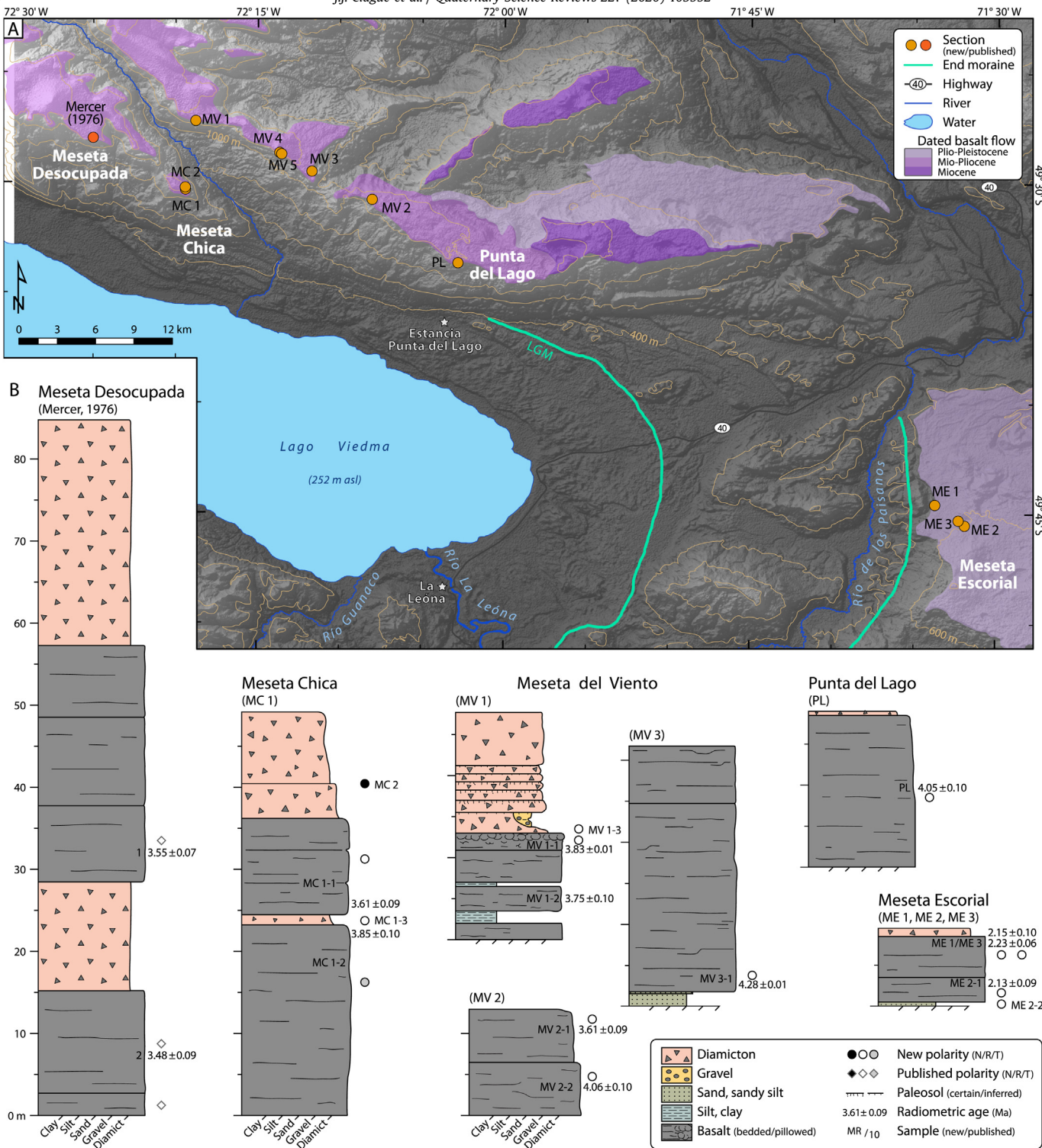


Fig. 4. Map (A) and stratigraphic sections (B) at mesetas Chica, Desocupada, del Viento, and Escorial, and Punta del Lago. Base map is derived from 1-arcsecond Shuttle Radar Topographic (SRTM v3) elevation data. Illustrated sections are for new sites described in this paper (see Table 1) and selected sites of Mercer (1976) and Schellmann (2000). Topographic contour interval is 200 m.

basaltic volcanic rocks; a few are striated. We interpret this sediment to be glaciolacustrine and to record a glacial event before about 2.2 Ma and likely well after the end of the normally magnetized Gauss Chron (2,608 Ma). The magnetization of the baked laminated sand is similar to that of the overlying basalt and is likely a thermal remagnetization at the time of flow emplacement. Given the absence of any evidence for quenching of the flow in a

water body, it is likely that the glaciolacustrine sand was deposited well before the eruption.

4.3. Early Pleistocene glacial deposits

Here we briefly summarize a published section at Cerro del Fraile to provide constraints on our interpretations of Pleistocene

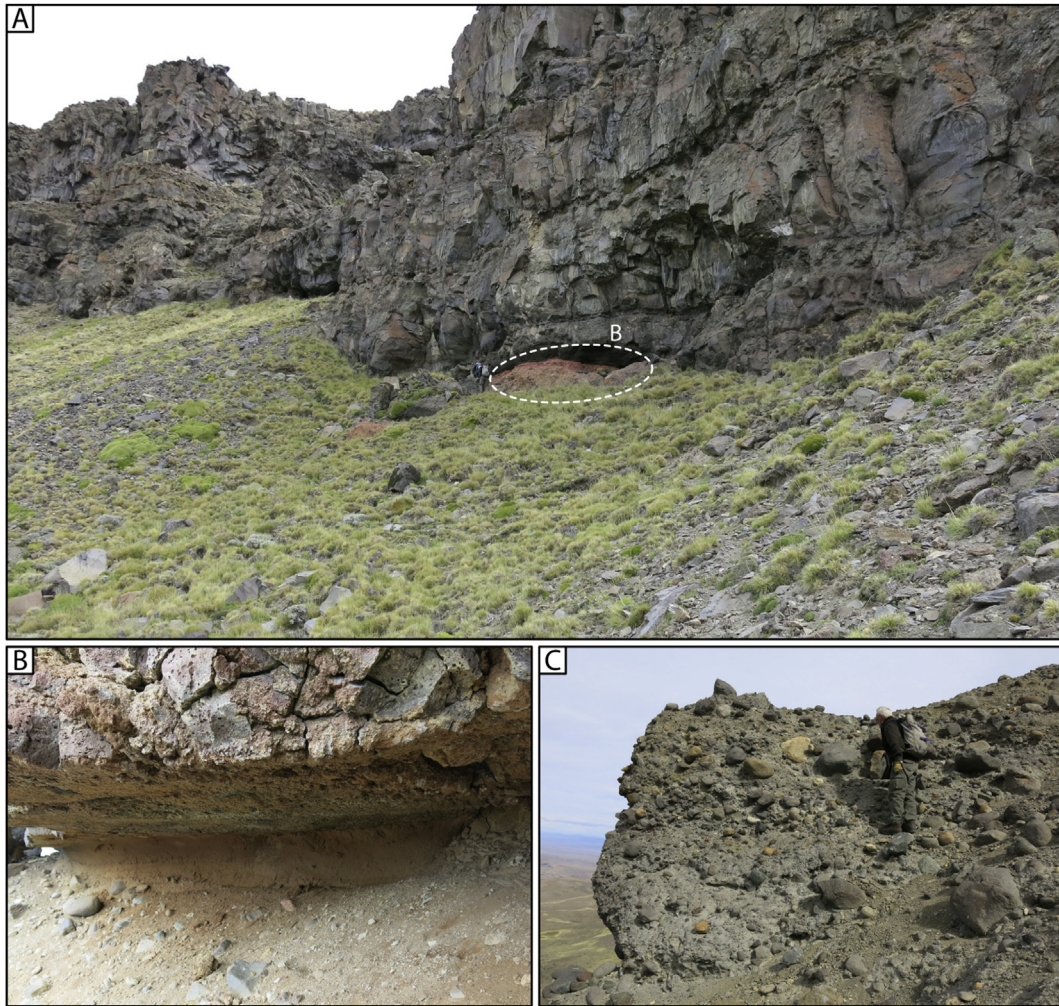


Fig. 5. A) Basalt flows separated by B) a till at the margin of Meseta Chica (site MC 1 in Fig. 4A). C) Till at the top of the flow sequence at this site. Note people for scale in A) and C).

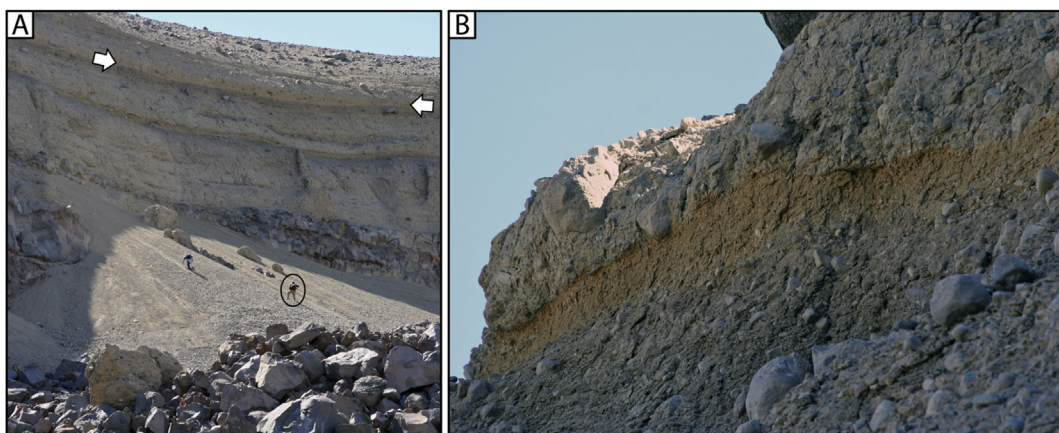


Fig. 6. A) Multiple tills separated by paleosols at Meseta del Viento (site MV 1 in Fig. 4A). The arrowed horizon is the paleosol shown in B. Note people for scale in A. The large partially sunlit boulder in B) is about 0.7 m in maximum diameter.

glaciation and landscape evolution. A 180-m-thick sequence of Early Pleistocene basalt flows containing seven discrete layers of till and glaciolacustrine sediment is exposed at Cerro del Fraile, south of Lago Argentino and southwest of El Calafate (Fig. 8; Fleck et al., 1972; Singer et al., 2004; and our observations). The sequence

unconformably overlies Late Cretaceous sedimentary rocks and extends up to 1200 m above the level of Lago Argentino. The lowest drift layer in the sequence underlies a basalt flow dated 2.18 ± 0.01 Ma. In sequence, the six drift layers above it date to about 2.2, 2.1, 2.0, 1.9, 1.4–1.8, and 1.0–1.6 Ma.

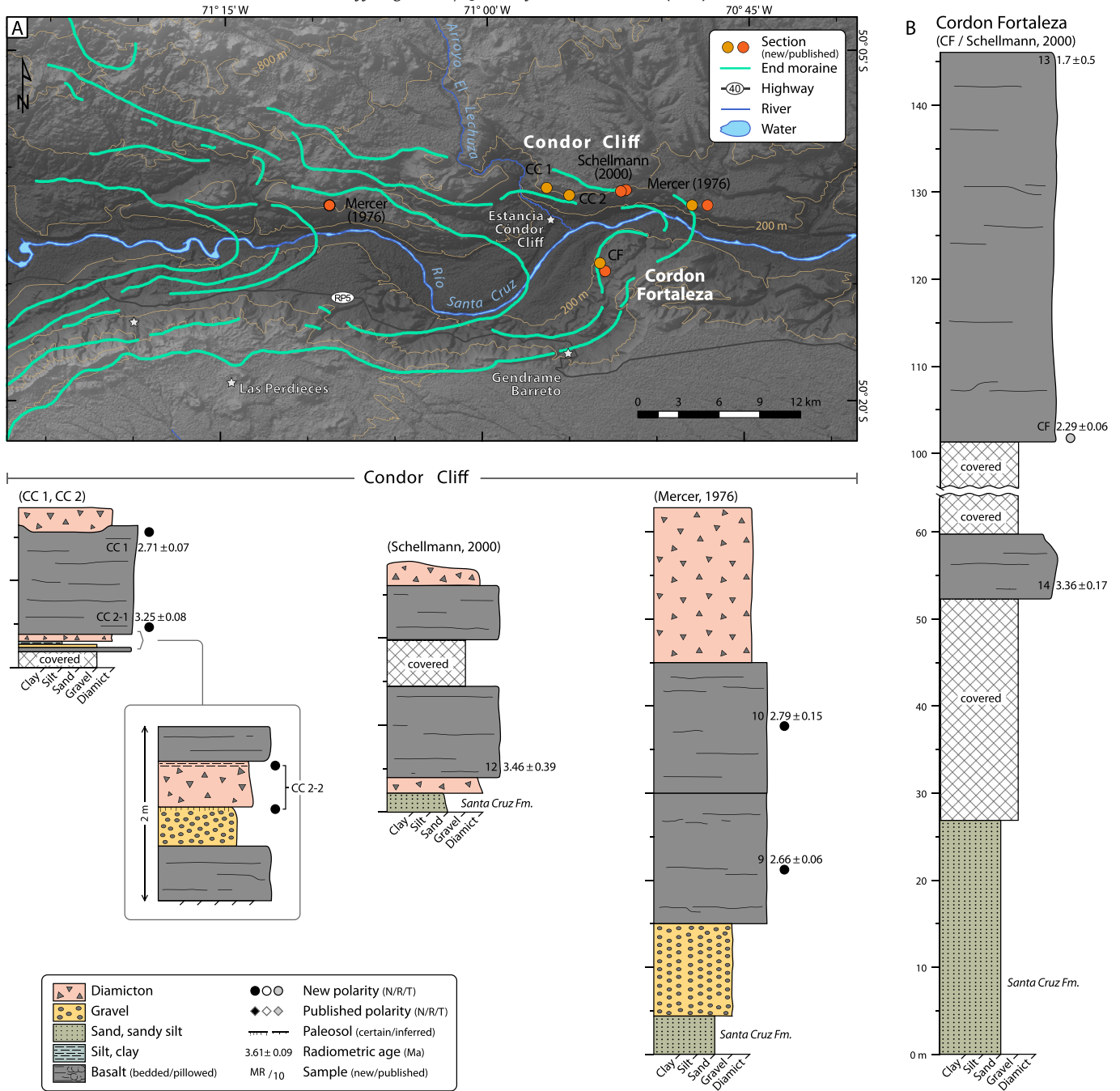


Fig. 7. Map (A) and stratigraphic sections (B) at Condor Cliff and Cordon Fortaleza. Base map is derived from 1-arcsecond Shuttle Radar Topographic (SRTM v3) elevation data. Illustrated sections are for new sites described in this paper (see Table 1) and selected sites of Mercer (1976) and Schellmann (2000). Topographic contour interval is 200 m.

Lateral and end moraines that are likely the same age as these glacial sediments are inset into the surfaces that preserve evidence of late Pliocene and earliest Pleistocene glaciations described above. Lateral moraines are nested between Lago Viedma and the surfaces of Meseta Chica and Meseta del Viento (Figs. 1 and 4; and our observations). These moraines become progressively more subdued and weathered with increasing elevation and distance from the Andes. Patches of high weathered till and erratics up to boulder size are present above the highest identified moraine, which is 250–400 m below the surfaces of Meseta Chica and Meseta del Viento. Similarly, eastward from the end of Lago Argentino along the valley of Río Santa Cruz (Figs. 7 and 8), end and lateral moraines become increasingly subdued and weathered.

The glaciations responsible for these valley-bottom moraines span the Pleistocene. Eight moraines cross the valley of Río Santa Cruz between the Marine Isotope Stage (MIS) 2 terminal moraine and Condor Cliff, a distance of about 55 km (Mercer, 1976). The absolute ages of the glaciations responsible for the pre-MIS 2 moraines are poorly known, although it is likely that some of the moraines are correlative with the Cerro del Fraile tills. Yet the number of end moraines that previous researchers have identified in the valley of the Río Santa Cruz and that span the period ca. 2.6 – 0.02 Ma (Mercer, 1976; Schellmann, 1998) is far fewer than the number of glaciations implied by the Cerro del Fraile sequence (seven events spanning the period 2.2–1.1 Ma). The latter record does not include the eight major 100 ka glacials of the past 800 ka because the

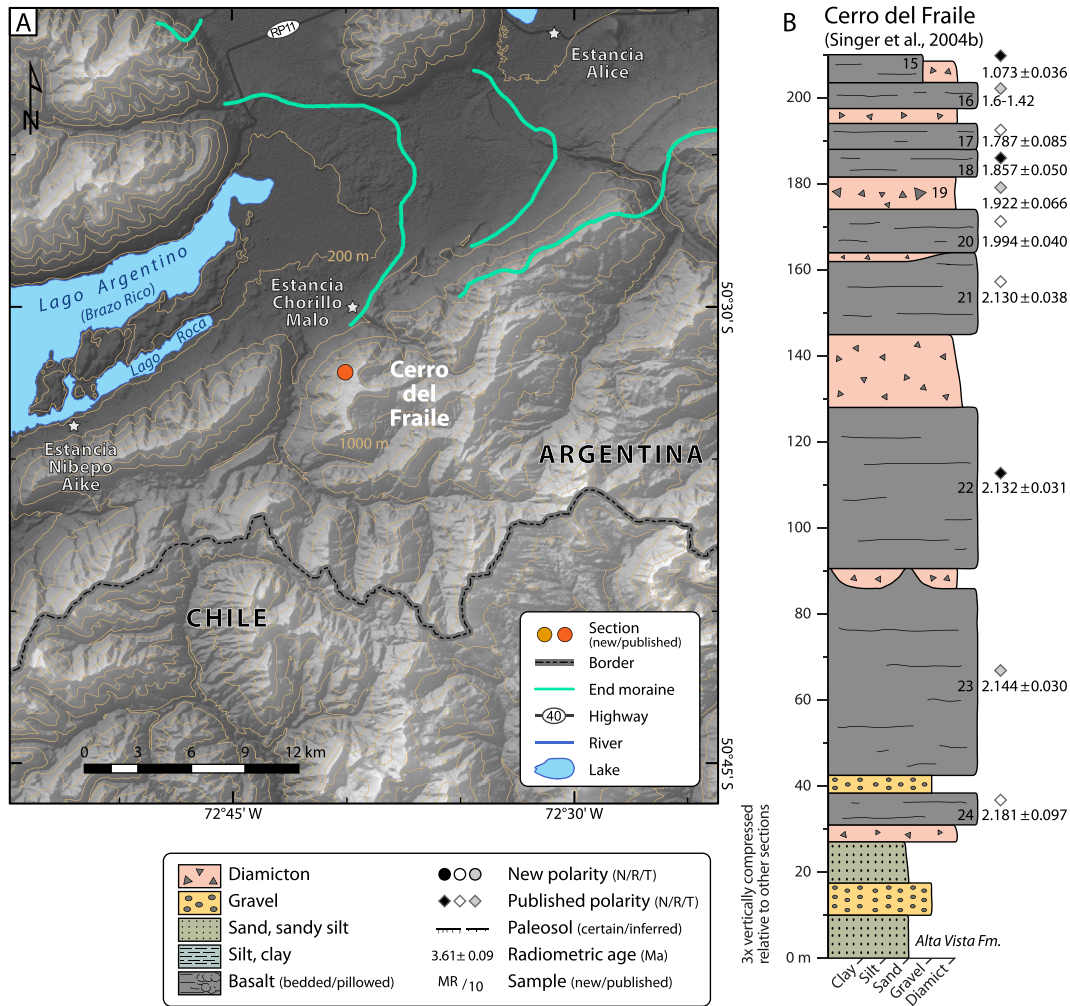


Fig. 8. Map (A) and stratigraphic section (B) at Cerro del Fraile. Base map is derived from 1-arcsecond Shuttle Radar Topographic (SRTM v3) elevation data. Section is modified from Singer et al., 2004. Topographic contour interval is 200 m.

youngest basalt flow at Cerro del Fraile is ca. 1 million years old. If we assume that each these 100 ka glacials left a deposit and moraine in the Santa Cruz valley east of Lago Argentino, fewer than half the inferred glacial events of the past 2.2 Ma have been identified to date.

5. Discussion

5.1. Pliocene and Early Pleistocene glacial record

The composite Pliocene and Early Pleistocene glacial record from our study area spans the period from about 3.6 Ma to 1 Ma (Fig. 8). It provides one of the most complete late Pliocene and Early Pleistocene terrestrial records of glaciation on Earth (Fig. 9). At least seven tills, separated by basalt flows or well developed paleosols, were deposited on the high mesetas north of Lago Viedma during the late Pliocene. Our ⁴⁰Ar/³⁹Ar ages suggest that one of these tills is approximately 3.7 Ma old; its age is roughly coincident with MIS events Gi2 and Gi4, both of which date to between 3.70 and 3.65 Ma (Lisiecki and Raymo, 2005). These events follow decreases in atmospheric CO₂ from 350 to 250 ppm at about 4.0 Ma (Bartoli et al., 2011) and are marked by short-lived increases in global ice volume. They also coincide with the onset of stadial conditions in the Patagonian Steppe (Amidon et al., 2017).

The ages of the seven till units at Meseta del Viento is unknown, but they all postdate 3.83 Ma and predate the Plio-Pleistocene transition. One or more of these tills were likely deposited soon after 3.3 Ma during global expansion of glaciers at that time (the prominent M2 MIS event of the MIS record). Unfortunately these sites lack upper basalt flows to help constrain the age range of these tills. In any case, patches of younger, highly weathered till and erratics are present on the upper slopes below these mesetas and are either latest Pliocene or Early Pleistocene in age. Similarly, remnants of what we interpret to be glaciogenic deposits between basalt flows at Condor Cliffs in the valley of Río Santa Cruz date to the Plio-Pleistocene transition, and Mercer (1976) identified and described till and glaciofluvial gravel about 275 m above the valley floor in this area. These deposits are the most easterly glacial deposits in this valley.

An additional seven drift units are present between basalt flows at Cerro del Fraile and can linked to cold periods between 2.2 Ma and 1.0 Ma in the astronomically tuned marine oxygen isotope record (Fig. 9). The outer limits of the glaciers that deposited these tills are unknown, but they lie far beyond the MIS 2 limit and thus likely relate, at least in part, to the outer series of terminal moraines mapped by Mercer (1976), Schellmann (1998), and Wenzens (2006) in the Río Santa Cruz valley east of Lago Argentino. Some of these glaciations also probably correspond to the Great Patagonian

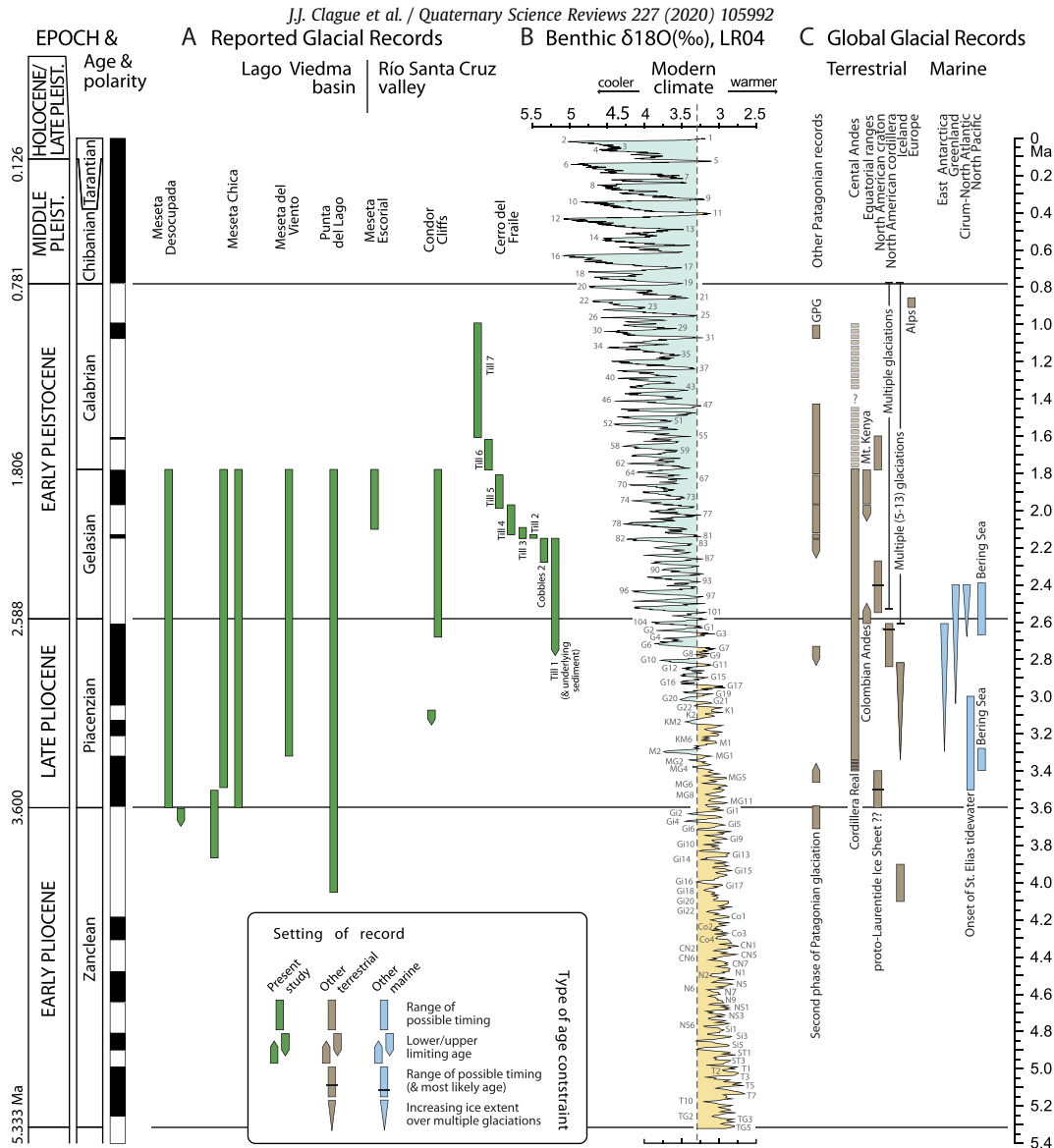


Fig. 9. A) Glacial record constrained temporally based on B) the Marine Isotope Stage time scale of [Lisiecki and Raymo \(2005\)](#), and compared with C) glacial records reported elsewhere. We have added two short-lived periods of normal polarity to the LR04 record, based on [Channell et al. \(2002\)](#); Gilsa event) and [Ogg \(2012\)](#); Reunion subchron). The LR04 benthic ^{18}O paleo-temperature profile is derived from 57 globally distributed records (conditions warmer than the Holocene mean in yellow, and those cooler than the Holocene mean in blue). Marine Isotope Stages (MIS) are labeled in grey (glacials as even numbers, interglacials as odd numbers). The MIS scheme follows [Lisiecki and Raymo \(2005\)](#) from the present (MIS 1) to the start of the Pleistocene (MIS 104) and [Shackleton et al. \(1995\)](#) for the Pliocene.

Glaciation, which is now known to encompass a series of glaciations, the youngest of which dates to about 1.1–1 Ma ([Meglioli, 1992](#); [Ton-That et al., 1999](#); [Singer et al., 2004a](#); [Griffing, 2018](#)).

Other late Pliocene ice caps existed in the eastern Bolivian Andes, southwest Yukon Territory, and Iceland (see [De Schepper et al., 2014](#) and [Roberts et al., 2018](#) for summaries). Exposures at La Paz, Bolivia, provide evidence for 11 late Pliocene glaciations, most of which are separated by interglacials of sufficient length to produce mature soils ([Roberts et al., 2017, 2018](#)). One latest Pliocene glaciation has been documented in Yukon Territory ([Froese et al., 2000](#); [Barendregt et al., 2010](#); [Duk-Rodkin et al., 2010](#); [Hidy et al., 2013](#)), whereas evidence for four Pliocene glaciations has been found in Iceland ([Helgason and Duncan, 2001](#); [Geirsdóttir, 2011](#)). Inferred Pliocene ice caps in northern Ontario ([Gao et al., 2012](#)) and southeastern Alaska ([Denton and Armstrong, 1969](#)) remain uncertain due to ambiguities in chronological control and the origin of diamicton units.

Glaciers extended eastward onto the meseta in the Lago Viedma area during the period 4.0–3.6 Ma, earlier than the oldest known ice caps farther north in the Central Andes near La Paz, Bolivia. The base of the Pliocene glacial sequence at La Paz is not exposed, however, and the earliest glaciations there may predate the oldest event (3.35 Ma) documented by [Roberts et al. \(2017, 2018\)](#). The record from these two sites provide the only evidence of glaciation in South America from the Piacenzian and Zanclean stages of the Pliocene.

The earliest parts of the Lago Viedma and La Paz glacial records substantially pre-date the earliest known late Cenozoic glaciation in the Colombian Andes (<2.6 Ma; [Helmens et al., 1997](#)) and on Mount Kenya (most likely 2.0–1.8 Ma; [Mahaney et al., 2013](#)). Additionally, they pre-date the onset of major, repeated tidewater glaciation adjacent to the Bering Sea ([Takahashi et al., 2011](#)) and North Atlantic ([Kleiven et al., 2002](#)) (ca. 2.7 Ma) and the first ice sheet in northwest North America ([Bailey et al., 2013](#); [Hidy et al.,](#)

2013) (ca. 2.7 Ma).

Numerous Early Pleistocene glaciations are known from Bolivia (six or more; Roberts et al., 2018), Yukon (up to seven; Barendregt et al., 2010), and Iceland (five to 13; Geirsdóttir, 2011). These numbers are broadly consistent with the Cerro del Fraile record of seven glaciations between 2.2 and 1.1 Ma, although it is not currently possible to correlate specific events among these sites.

5.2. Plio-Pleistocene landscape evolution

The dated basalt flows forming the mesetas in the Lago Viedma area also provide information about landscape evolution in the area. Individual flows are thin but cover relatively large areas, and were thus emplaced by highly fluid outpourings of magma from cones and vents. The flows and the mesetas on which they sit dip gently to the east away from the front of the Andes and have not been noticeably tilted since their emplacement. The close agreement of the overall mean magnetic directions of the widely spaced basalt flows and sediments that we sampled with the GAD field supports this inference (Supplement Fig. S3). The mapped extent of the flows shows that they erupted onto a pediment surface of low to moderate relief; there is no evidence that the flows were channeled into deep paleo-valleys. Streams flowed from the Andes towards the Atlantic Ocean over a landscape with much lower relief than today (Fig. 10A). The flow sequences terminate abruptly in escarpments at the sides of Lago Viedma and Lago Argentino, and these depressions are clearly younger than the mesetas and the basalts that cap them.

We argue that a series of Early and Middle Pleistocene glaciers formed and deepened the great valley of Lago Viedma, stranding the late Pliocene mesetas high above its floor (Fig. 10B). This inference is consistent with an argument made by Anderson et al. (2012) that erosion during repeated glaciations might account for a long-term reduction in glacier extent, resulting in the preservation of end moraines from a long sequence of late Cenozoic glaciations. This concept was proposed earlier by Kaplan et al. (2009) based on differences between the latest Early Pleistocene limit (Great Patagonian Glaciation) and the Last Glacial limit in Patagonia. Here we provide support for this concept with our inferences about ice extent during glacials extending from the late Pliocene to the Middle Pleistocene. In our case, vertical incision of the landscape provided accommodation space for Pleistocene valley glaciers and preserved patches of Pliocene till on high pediments. Vertical erosion also helps explain the apparent paradox between the high elevations of the late Pliocene tills relative to Middle and Late Pleistocene moraines in the study area and the increasing intensity of glaciation over the past 3.7 Ma. The volume of ice involved in the late Pliocene advances may have been smaller than that sourced from the Andes during the Middle and Late Pleistocene.

The importance of glacier erosion and its ability to incise the landscape could also explain the age-elevation relation of glacier deposits found in the vicinity of Lago Argentino. The lake sits within a glacially over-deepened valley bordered by the high, flat-lying, 2.2–1.1 Ma basalt flows of Cerro del Fraile (Fig. 7). The oldest of these flows rests on a thin till and about 15 m of fluvial or glacio-fluvial sand and gravel, which in turn rest on Cretaceous bedrock at 1020 m asl, about 840 m above the surface of Lago Argentino. Given the topographic setting, we conclude that the Lago Argentino depression began to develop before 2.2 Ma. Farther east near Condor Cliff, Río Santa Cruz was flowing in a channel nested within flanking basalt-covered mesetas as early as the Early Pleistocene. We base this interpretation on the presence of a ca. 2.7 Ma flow lying on an early Miocene bedrock strath about 100 m above the valley floor near Condor Cliff. Comparable dissection of a low- to

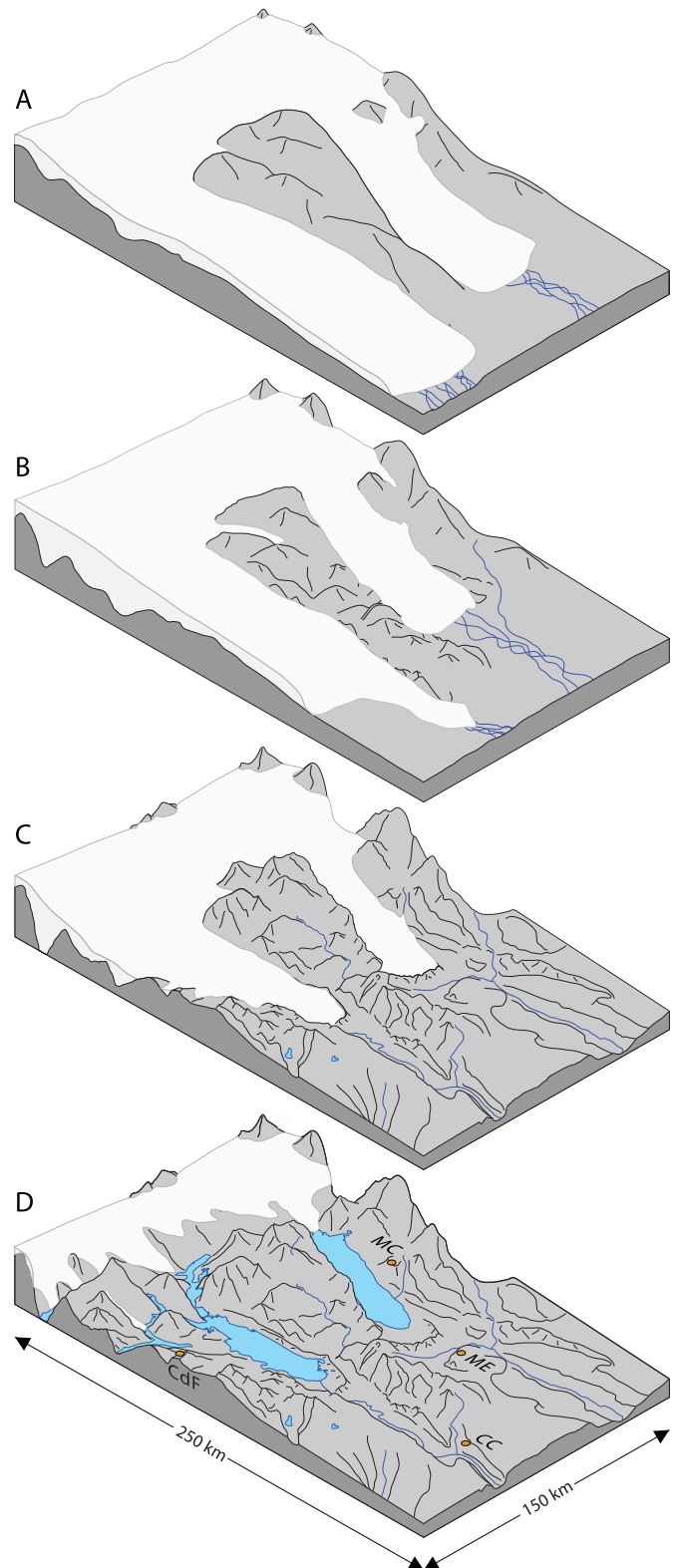


Fig. 10. Schematic diagrams showing the landscape of the Lago Viedma/Lago Argentino area at four different times: A) A latest Pliocene or earliest Pleistocene glaciation; B) a Middle Pleistocene glaciation; C) the Last Glacial Maximum; and D) the Holocene, when the landscape had attained its present form.

moderate-relief landscape since the Pliocene has been documented in the Lago Buenos Aires area on the east side of the Andes 335 km north of Lago Viedma (Lagabrielle et al., 2010; Scalabrino et al., 2011), although those authors hypothesized that it was driven by extensional tectonics related to subduction of the South Chilean spreading ridge and the related development of an asthenospheric slab window beneath Patagonia.

Glacial erosion and incision of the central Andes and the adjacent Patagonian Steppe probably coincided with similar changes to the landscape of the cordilleras of the Northern Hemisphere. Much of this erosion apparently was accomplished during the Middle and Late Pleistocene when major glacial cycles spanned approximately 100 ka and were longer and stronger than earlier glacials.

6. Conclusion

We summarize evidence for Pliocene and Early Pleistocene glaciation and landscape evolution in Southern Patagonia based on a review of relevant literature, field investigations, $^{40}\text{Ar}/^{39}\text{Ar}$ dating of basalt flows, and paleomagnetic analysis of basalts and sediments. Deposits of at least seven Pliocene and earliest Pleistocene glaciations, spanning the period from about 3.7 Ma to shortly after 2.6 Ma, are present on the mesetas north, east, southeast of Lago Viedma. During each of these events, an ice cap was present over the crest of the Andes and fed piedmont glaciers that flowed at least 80 km to the east over a low-relief surface that sloped gently towards the South Atlantic. An additional seven Early Pleistocene glaciations are recorded by tills interlayered with basalt flows in the north-facing escarpment of Cerro del Fraile, south of Lago Argentino. These events range in age from 2.2 Ma to about 1.1 Ma. The 14 Pliocene and Early Pleistocene glaciations recorded in the basalt-bounded meseta sequences provide one of the longest continental records of Cenozoic glaciation. The Patagonian record overlaps the 1.5-Ma-long record of Plio-Pleistocene glaciation recently reported from the eastern Central Andes in Bolivia, but spans as much as 1 Ma of additional time.

Basalt flows and lateral and end moraines of Early to Late Pleistocene age lie within the large, glacially eroded troughs that today host Lago Viedma, Lago Argentino, and Río Santa Cruz. Their age and distribution show that a low-relief late Pliocene pediment east of the Andes was deeply incised by glaciers and meltwater during the Pleistocene.

Acknowledgements

This research was supported by the Natural Sciences and Engineering Research Council (NSERC) through Discovery Grants to Barendregt, Clague, and Menounos (grant numbers 0581, 24595, and 05639), and Canada Research Chair (CRC) funds to Clague and Menounos. We thank journal reviewers Philip Gibbard and Ronald Rodbell for their thoughtful and helpful comments on an earlier version of the paper.

Appendix A. Supplementary data

Supplementary data to this article can be found online at <https://doi.org/10.1016/j.quascirev.2019.105992>.

References

- Amidon, W.H., Fisher, G.B., Burbank, D.W., Ciccioli, P.L., Alonso, R.N., Gorin, A.L., Silverhart, P.H., Kylander-Clark, A.R.C., Christoffersen, M.S., 2017. Mio-Pliocene aridity in the south-central Andes associated with Southern Hemisphere cold periods. *Proc. Natl. Acad. Sci.* 114, 6474–6479.
- Anderson, R.S., Dühnforth, M., Colgan, W., Anderson, L., 2012. Far-flung moraines: exploring the feedback of glacial erosion on the evolution of glacier length. *Geomorphology* 179, 269–285.
- Bailey, I., Hole, G.M., Foster, G.L., Wilson, P.A., Storey, C.D., Trueman, C.N., Raymo, M.E., 2013. An alternative suggestion for the Pliocene onset of major northern hemisphere glaciation based on the geochemical provenance of North Atlantic Ocean ice-rafted debris. *Quat. Sci. Rev.* 75, 181–194.
- Barendregt, R.W., Enkin, J.E., Duk-Rodkin, A., Baker, J., 2010. Paleomagnetic evidence for multiple late Cenozoic glaciations in the Tintina Trench, west-central Yukon, Canada. *Can. J. Earth Sci.* 47, 987–1002.
- Bartoli, G., Hönisch, B., Zeebe, R.E., 2011. Atmospheric CO₂ decline during the Pliocene intensification of northern hemisphere glaciations. *Paleoceanography* 26, PA4213. <https://doi.org/10.1029/2004PA001071>.
- Butler, R.F., 1992. *Paleomagnetism: Magnetic Domains to Geologic Terranes*. Blackwell Scientific Publications, Boston, MA.
- Channell, J.E.T., Mazaud, A., Sullivan, P., Turner, S., Raymo, M.E., 2002. Geomagnetic excursions and paleointensities in the Matuyama Chron at Ocean Drilling Program Sites 983 and 984 (Iceland Basin). *J. Geophys. Res.* 107 (B6), 2114. <https://doi.org/10.1029/2001JB000491>.
- Clapperton, C.M., 1979. Glaciation in Bolivia before 3.27 Myr. *Nature* 277, 375–377.
- Coutand, I., Diraison, M., Cobbold, P.R., Gapais, D., Rossello, E.A., Miller, M., 1999. Structure and kinematics of a foothills transect, Lago Viedma, southern Andes (49°30'S). *J. South Am. Earth Sci.* 12 (1), 1–15.
- Dalrymple, B., Alexander, E.C., Lamphere, M.A., Kraker, G.P., 1981. Radiation of Samples for $^{40}\text{Ar}/^{39}\text{Ar}$ Dating Using the Geological Survey TRIGA Reactor. U.S. Geological Survey Professional Paper 1176, 55 pp.
- De Schepper, S., Gibbard, P.L., Salzmann, U., Ehlers, J., 2014. A global synthesis of the marine and terrestrial evidence for glaciations during the Pliocene Epoch. *Earth Sci. Rev.* 135, 83–102.
- Denton, G.H., Armstrong, R.L., 1969. Miocene-Pliocene glaciations in southern Alaska. *Am. J. Sci.* 267, 1121–1142.
- Duk-Rodkin, A., Barendregt, R.W., White, J.W., 2010. An extensive late Cenozoic terrestrial record of multiple glaciations preserved in the Tintina Trench of west-central Yukon; stratigraphy, paleomagnetism, paleosols, and pollen. *Can. J. Earth Sci.* 47, 1003–1028.
- Eyles, C.H., Eyles, N., 1989. The upper Cenozoic White River “tillites” of southern Alaska: subaerial slope and fan-delta deposits in a strike-slip setting. *Geol. Soc. Am. Bull.* 101, 1091–1102.
- Feruglio, E., 1944. Estudios Geológicos y Glaciológicos en la Región del Lago Argentino (Patagonia). *Boletín Academia Nacional Ciencias de Córdoba* 37, 208 pp.
- Fleck, R.J., Mercer, J.H., Nairn, A.E.M., Peterson, D.N., 1972. Chronology of late Pliocene and early Pleistocene glacial and magnetic events in southern Argentina. *Earth Planet. Sci. Lett.* 16, 15–22.
- Forsythe, R.D., Nelson, E.P., Carr, M.J., Kaeding, M.E., Herve, M., Mpodozis, C., Soffia, J.M., Harambour, S., 1986. Pliocene near-trench magmatism in southern Chile; a possible manifestation of ridge collision. *Geology* 14, 23–27.
- Froese, D.G., Barendregt, R.W., Enkin, R.J., Baker, J., 2000. Paleomagnetic evidence for multiple late Pliocene – early Pleistocene glaciations in the Klondike area, Yukon Territory. *Can. J. Earth Sci.* 37, 863–877.
- Gao, C., McAndrews, J.H., Wang, X., Menzies, J., Turton, C.L., Wood, B.D., Pei, J., Kodors, C., 2012. Glaciation of north America in the James Bay Lowland, Canada, 3.5 Ma. *Geology* 40, 975–978.
- Geirsdóttir, Á., 2011. Pliocene and Pleistocene glaciations of Iceland: a brief overview of the glacial history. In: Ehlers, J., Gibbard, P.L., Hughes, P. (Eds.), *Quaternary Glaciations—Extent and Chronology: A Closer Look*, vol. 15. Elsevier Developments in Quaternary Science, pp. 199–210.
- Gorring, M.L., 2008. Field-trip guide: ridge-trench collision – the southern Patagonian Cordillera east of the Chile triple junction. In: Mahlborg Kay, S., Ramos, V.A. (Eds.), *Field Trip Guides to the Backbone of the America in the Southern and Central Andes: Ridge Collision, Shallow Subduction, and Plateau Uplift*, vol. 13. Geological Society of America, Field Guide, pp. 1–22.
- Gorring, M.L., Kay, S.M., 2001. Mantle processes and sources of Neogene slab window magmas from southern Patagonia, Argentina. *J. Petrol.* 42, 1067–1094.
- Gorring, M.L., Kay, S.M., Zeitler, P.K., Ramos, V.A., Rubiolo, D., Fernandez, M.L., Panza, J.L., 1997. Neogene Patagonian plateau lavas: continental magmas associated with ridge collision at the Chile Triple Junction. *Tectonics* 16, 1–17.
- Griffing, C.Y., 2018. Late Cenozoic Glaciations and Environments in Southernmost Patagonia. Ph.D. thesis. Simon Fraser University, Burnaby, BC, 193 pp.
- Haug, G.H., Tiedemann, R., 1998. Effect of the formation of the Isthmus of Panama on Atlantic Ocean thermohaline circulation. *Nature* 393, 673–676.
- Helgason, J., Duncan, R.D., 2001. Glacial-interglacial history of the Skaftafell region, southeast Iceland, 0–5 Ma. *Geology* 29, 179–182.
- Helmens, K.F., Barendregt, R.W., Enkin, R.J., Baker, J., Andriessen, P.A.M., 1997. Magnetic polarity and fission-track chronology of late Pliocene–Pleistocene paleoclimatic proxy record in the tropical Andes. *Quat. Res.* 48, 15–28.
- Hidy, A.J., Gosse, J.C., Froese, D.G., Bond, J.D., Rood, D.H., 2013. A latest Pliocene age for the earliest and most extensive Cordilleran Ice Sheet in northwestern Canada. *Quat. Sci. Rev.* 61, 77–84.
- Hill, D.J., Bolton, K.P., Haywood, A.M., 2017. Modelled ocean changes at the Plio-Pleistocene transition driven by Antarctic ice advance. *Nat. Commun.* 8 <https://doi.org/10.1038/ncomms14376>.
- Kaplan, M.R., Hein, A.S., Hubbard, A., Lax, A.M., 2009. Can glacial erosion limit the extent of extent of glaciation? *Geomorphology* 103, 172–179.
- Kirschvink, J.L., 1980. The least-squares line and plane and the analysis of paleomagnetic data. *Geophys. J. R. Astron. Soc.* 62, 699–718.
- Kleiven, H.F., Jansen, E., Fronval, T., Smith, T.M., 2002. Intensification of northern

- hemisphere glaciations in the circum Atlantic region (3.5–2.4 Ma) – ice-rafted detritus evidence. *Palaeogeogr. Palaeoclimatol. Palaeoecol.* 184, 213–223.
- Kuiper, K.F., Deino, A., Hilgen, F.J.W., Krijgsman, Renne, P.R., Wijbrans, J.R., 2008. Synchronizing rock clocks of Earth history. *Science* 320, 500–504.
- Lagabrielle, Y., Scalabrino, B., Suárez, M., Ritz, J.-F., 2010. Mio-Pliocene glaciations of Central Patagonia; new evidence and tectonic implications. *Andean Geol.* 37, 276–299.
- Lee, J.-Y., Marti, K., Severinghaus, J.P., Kawamura, K., Yoo, H.-S., Lee, J.B., Kim, J.S., 2006. A redetermination of the isotopic abundances of atmospheric Ar. *Geochim. Cosmochim. Acta* 70, 4507–4512.
- Lisiecki, L.E., Raymo, M.E., 2005. A Pliocene-Pleistocene stack of 57 globally distributed benthic $\delta^{18}\text{O}$ records. *Paleoceanography* 20, PA1003. <https://doi.org/10.1029/2004PA001071>.
- Lunt, D.J., Foster, G.L., Haywood, A.M., Stone, E.J., 2008. Late Pliocene Greenland glaciation controlled by a decline in atmospheric CO_2 levels. *Nature* 454, 1102–1105.
- Mahaney, W.C., Barendregt, R.W., Hamilton, T.S., Hancock, R.G.V., Tessler, D., Costa, J.M., 2013. Stratigraphy of the Gorges moraine system, Mount Kenya: Palaeosol and palaeoclimate record. *J. Geol. Soc. Lond.* 170, 497–511.
- Meglioli, A., 1992. Glacial Geology and Chronology of Southernmost Patagonia and Tierra del Fuego, Argentina and Chile. PhD thesis. Lehigh University, Bethlehem, PA.
- Mercer, J.H., 1976. Glacial history of southernmost South America. *Quat. Res.* 6, 125–166.
- Mercer, J.H., 1983. Cenozoic glaciation in the southern hemisphere. *Annu. Rev. Earth Planet Sci.* 11, 99–132.
- Mercer, J.H., Fleck, R.J., Mankinen, E.A., Sander, W., 1973. Southern Patagonia: glacial events between 4 m.y. and 1 m.y. ago. In: Suggate, R.P., Cresswell, M.M. (Eds.), *Quaternary Studies*. Royal Society of New Zealand, Wellington, pp. 223–230.
- Murdie, R., Prior, D.J., Styles, P., Flint, S.S., Pearce, R.J., Agar, S.M., 1993. Seismic responses to ridge-transform subduction; Chile triple junction. *Geology* 21, 1095–1098.
- Ogg, J.G., 2012. Geomagnetic polarity time scale – Chapter 5. In: Gradstein, F., Ogg, J.G., Schmitz, M., Ogg, G. (Eds.), *The Geologic Time Scale 2012*. Elsevier, Amsterdam, pp. 85–113.
- Rabassa, J., 2008. Late Cenozoic glaciations in Patagonia and Tierra del Fuego. In: Rabassa, J. (Ed.), *Late Cenozoic of Patagonia and Tierra del Fuego*, vol. 11. Elsevier Developments in Quaternary Science, pp. 151–204.
- Ramos, V.A., 1989. Andean foothills structures in northern Magallanes Basin, Argentina. *AAPG (Am. Assoc. Pet. Geol.) Bull.* 73, 887–903.
- Ramos, V.A., Ghiglione, M.C., 2008. Tectonic evolution of the Patagonian Andes. In: Rabassa, J. (Ed.), *Late Cenozoic of Patagonia and Tierra del Fuego*, vol. 11. Elsevier Developments in Quaternary Sciences, pp. 57–71.
- Ramos, V.A., Kay, S.M., 1992. Southern Patagonian plateau basalts and deformation: backarc testimony of ridge collisions. *Tectonophysics* 205, 261–282.
- Riccardi, A.C., 1988. The Cenozoic system of southern south America. *Geol. Soc. Am. Mem.* 168, 161 pp.
- Roberts, N.J., Barendregt, R.W., Clague, J.J., 2017. Multiple tropical Andean glaciations during a period of late Pliocene warmth. *Sci. Rep.* 7, 41878, 9 pp.
- Roberts, N.J., Barendregt, R.W., Clague, J.J., 2018. Pliocene and Pleistocene chronostratigraphy of continental sediments underlying the Altiplano at La Paz, Bolivia. *Quat. Sci. Rev.* 189, 105–126.
- Ruddiman, W.F., Kutzbach, J.E., 1989. Forcing of late Cenozoic Northern Hemisphere climate by plateau uplift in southern Asia and the American west. *J. Geophys. Res.* 94 (D15), 18409–18427.
- Scalabrino, B., Ritz, J.-F., Lagabrielle, Y., 2011. Relief inversion triggered by subduction of an active spreading ridge: evidence from glacial morphology in Central Patagonia. *Terra. Nova* 23, 63–69.
- Schellmann, G., 1998. Jungkinozoische Landschaftsgeschichte Patagoniens (Argentinien). *Andine Vorlandvergletscherungen, Talentwicklung und marine Terrassen*. Essener Geographische Arbeiten 29, 216 pp.
- Schellmann, G., 2000. Landscape evolution and glacial history of Southern Patagonia (Argentina) since the late Miocene – some general aspects. *Zentrablatt für Geologie und Paläontologie Teil I* 1013–1026.
- Shackleton, N.J., Hall, M.A., Pate, D., 1995. Pliocene stable isotope stratigraphy of ODP Site 846. In: *Proceedings of the Ocean Drilling Program – Scientific Results*, vol. 138, pp. 337–356.
- Singer, B.S., Ackert Jr., R.P., Guillou, H., 2004a. $^{40}\text{Ar}/^{39}\text{Ar}$ and K-Ar chronology of Pleistocene glaciations in Patagonia. *Geol. Soc. Am. Bull.* 116, 434–450.
- Singer, B.S., Brown, L.L., Rabassa, J.O., Guillou, H., 2004b. $^{40}\text{Ar}/^{39}\text{Ar}$ late Pliocene and early Pleistocene geomagnetic and glacial events in southern Argentina. In: Channel, J.E.T., Kent, D.V., Lowrie, W., Meert, J.G. (Eds.), *Geophysical Monograph*, 145. American Geophysical Union, pp. 175–190.
- Strehlin, J.A., 1995. New evidence on the relationships of the oldest extra-Andean glaciations in the Río Santa Cruz area. In: *Quaternary of South America and Antarctic Peninsula*. A.A. Balkema, Rotterdam/Boston, vol. 9, pp. 105–116.
- Takahashi, K., Ravelo, A.C., Alvarez Zarikian, C., IODP Expedition 323 Scientists, 2011. IODP expedition 323 – Pliocene and Pleistocene paleoceanographic changes in the Bering Sea. *Sci. Drill. J.* 11, 4–13.
- Ton-That, T., Singer, B., Möner, N.A., Rabassa, J., 1999. Datación por el método $^{40}\text{Ar}/^{39}\text{Ar}$ de lavas basálticas y geología del Cenozoico Superior en la región del Lago Buenos Aires, provincia de Santa Cruz, Argentina. *Asociación Geológica Argentina, Revista* 54, 333–352.
- Wenzens, G., 2000. Pliocene piedmont glaciation in the Río Shehuen valley, southeast Patagonia, Argentina. *Arctic Antarct. Alpine Res.* 32, 46–54.
- Wenzens, G., 2006. Terminal moraines, outwash plains, and lake terraces in the vicinity of Lago Cardiel (49°S; Patagonia, Argentina) – evidence for Miocene Andean foreland glaciation. *Arctic Antarct. Alpine Res.* 38, 276–291.
- Wenzens, G., Wenzens, E., Schellmann, G., 1996. Number and types of piedmont glaciations east of the central southern Patagonian Icefield. *Zentrablatt für Geologie und Paläontologie Teil I* 779–790.
- Wenzens, G., Wenzens, E., Schwan, H., Schellmann, G., 1998. Vorlandvergletscherungen östlich des Lago Viedman (Südpatagonien) und ihre Erfassung in Satellitenbildern. *Satellitenbildern*. In: Gossman, H. (Ed.), *Geowissenschaftliche Forschungen in der Antarktis und in Südpatagonien mit ERS-1-Radarbildern*. Gotha: Petermanns Geographische Mitteilungen, Ergänzungsheft, vol. 287, pp. 145–161.